Supporting Information

Ferring et al. 10.1073/pnas.1106638108

SI Text

Geology. This section and the details in Table S1 provide a detailed profile description for the M5 section, a summary of key soil morphological properties (Table S2), and additional discussion of the geology and site formation setting.

Sedimentary and pedogenic features of the stratum A deposits indicate an overall favorable site formation setting (Table S2). Pedogenic features show the immature soils in stratum A deposits compared with those in stratum B. Stratum A1 was buried by stratum A2a deposits before soils could develop, indicating that the artifacts in that stratum must have been deposited shortly after cooling of the Masavera Basalt and its burial by stratum A1 ashes. Longer periods of surface stability for stratum A2 deposits are shown by more soil structure and clay films, which may have contributed to the higher artifact densities in those strata, compared with strata A3 and A4 (Fig. 2).

In strata A4 and A3, evidence for bioturbation includes fine (<1.5-cm diameter) vertical burrows probably created by insects and 2- to 3-cm krotovina excavated by micromammals. However, the fills of the krotovina are very distinct from the surrounding matrix, and none of the 54 artifacts mapped in situ were found in those features. Only three of the flake fragments from stratum A4 were small enough to have been moved in burrows, but, despite differences in raw materials, the remote possibility for their biogenic introduction from stratum B1 cannot be excluded. The many fine pores in strata A2a–A4b are characteristic of soils formed in young ashes (1); the preservation of pores as well as the absence of any shrink–swell features indicates that soil turbation did not promote vertical displacement of artifacts. Importantly, the artifacts range in size from small flakes 2.0–2.5 cm long up to a 12.1-cm brown tuff core, supporting evidence for the fact that the stratum A archaeological horizons register serial living surfaces.

At the stratum A/B contact in the M5 section, A4 sediments have been truncated by minor erosion, with a lag of rare granules and pebbles. There are small rip-ups of the A4 sediments within the lower part of B1, which is a pale yellowish brown silt ash dominated by clear glass shards and small glass spheres. This unit, like stratum B3 above, was rapidly invaded by micromammals, most probably migratory hamsters (*Cricetulus* sp.) and gerbils (*Parameriones* aff. *Obeidiyensis*), which together comprise ~80% of the rodent fauna. Their burrowing activity is indicated by many burrows (krotovina) within the freshly deposited ashes that penetrate into the underlying sediments. The B1 ashes in M5 also have distinctive laminated calcretes, which are present in all exposures across the site except in the M6 section (Fig. 1). These and higher calcretes retarded or arrested water percolation, contributing to the excellent preservation of fossils in the main excavation areas.

Stratum B2 is composed of ashes having basal matrix–supported colluvial pebbles and cobbles, apparently derived from nearby terrace deposits. The B2 surface was stabilized long enough for moderate to strong soil development, indicated by an argillic horizon that was later intensively bioturbated and calcified, leaving the pedorelicts (Fig. 2). Stratum B2, in turn, is overlain by the fresh B3 ashes and then the B4 ashes, which have a well-developed argillic horizon and Stage II–III pedogenic carbonates, including a surmounting nodular and laminated caliche (indurated soil carbonate). Stratum B5 sediments are silt loams of a very different character than all sediments below and appear to be eolian. A strongly developed soil formed in these deposits, with a thick argillic horizon and pedogenic carbonates with a "ladder-backed" fabric (2), indicating a prolonged period of soil formation. In sum, the progressively stronger expression of soil morphology in strata B1–B5 deposits indicates that the entire suite of deposits was characterized by waning rates of episodic deposition, separated by increasingly long periods of stability and weathering.

Mineralogical Discussion. The estimated frequencies of crystalline mineral phases for the M5 sedimentary sequence is summarized in Fig. S2. Throughout the entire sequence, the most abundant crystalline mineral phase is represented by the feldspars, principally plagioclase. Olivine is only present in the Masavera Basalt and the A1a black ash. Pyroxenes are present in the basalt and in the sediments of strata A1–A3. The absence of pyroxenes above stratum A3 is presumably because of weathering, although possible changes in sediment sources need to be investigated further. Clay minerals are mainly composed of randomly interstratified mica-smectite, random smectite, and hydroxy-interlayered smectite with moderately polymerized Al-hydroxyls and kaolinite.

The black stratum A1a ashes have composition very similar to that of the underlying Masavera Basalt, suggesting a possible common source. The presence of olivine and the absence of carbonates and clay minerals in both the basalt and the A1a ashes is evidence for rapid burial and minimal weathering. The presence of clay minerals and calcite in the A2 sediments support the field evidence for cyclical surface stability, vegetative cover, and soil formation. These are the first deposits that register human occupation. The parent material of the A4 layer and the B sediment sequence underwent more weathering and associated pedogenesis compared with the underlying layers as shown by the absence of pyroxenes and the formation of clay minerals.

Artifact Descriptions. The dorsal cortex and scar patterns for flakes from M5 are shown in Tables S2 and S3. These show the low frequency of cortical pieces and the more complex scar patterns among flakes from stratum A compared with those from stratum B.

SI Methods

Archeology. After the initial discovery of artifacts in stratum A2 deposits, all excavated sediment was screened through 3-mm mesh. During excavation of the expanded 2 × 1.9-m test, excavations were conducted following the natural stratigraphy. All deposits were screened, and all artifacts found in situ were mapped in three dimensions. Attributes of all artifacts, including platform, dorsal scar patterns, dorsal cortex, and metrics were recorded. Summaries of scar patterns and dorsal cortex for the stratum A and stratum B combined assemblages are shown in Tables S3 and S4.

Paleomagnetism. One to four samples were obtained from each studied horizon to undergo magnetostratigraphic study. All samples were collected by hand, after exposure of fresh sediment that was oriented with a magnetic compass.

Remanent magnetization measurements were carried out with a 2G Enterprises high-resolution cryogenic magnetometer with superconducting quantum interference device (SQUID) sensors at the Paleomagnetism Laboratory of the Scientific Technical Services of Barcelona University. After measuring the natural remanent magnetization, a stepwise demagnetization was applied at least to one specimen per horizon. Demagnetization of 99 samples was done thermally because it was observed to be an efficient method in previous studies (3). A stepwise demagnetization from room temperature to 600 °C was accomplished, generally with an 8- to 10-step protocol.

Mineralogy. The bulk mineralogical composition of the sediments was characterized by integrating elemental analysis by X-ray fluorescence, X-ray diffractometry, and FTIR spectroscopy. Major element composition (Si, Ti, Al, Fe, Mn, Mg, Ca, Na, K, and P) were obtained on fused La-bearing lithium borate glass disks using a Siemens MRS-400 multichannel, simultaneous X-ray spectrometer. X-ray diffractometry analysis was carried out with a Philips X'Pert diffractometer, with Cu kα radiation (tube settings: 40 kV and 30 mA measuring in the range of 3–60° 2θ, at a rate of 0.02° per min). Representative FTIR spectra were obtained by grinding a few tens of micrograms of sample with an agate mortar and pestle and suspended with ~80 mg of KBr (IR grade). A 7-mm pellet was made by using a hand press (Qwik Handi-Press; Spectra-Tech Industries Corporation) without evacuation. The spectra were collected between 4,000 and 400 cm^{-1} at 4-cm^{-1} resolution with a Thermo-Nicolet Nexus 470 IR spectrometer.

The clay size fraction of each sample was obtained by pretreating the sediments in solutions of hydrogen peroxide (H_2O_2) and sodium hydroxide (NaOH). The resulting silt fractions were then dispersed both at pH 4 (HCl solution) and at pH 10 (NaOH solution). The clay fractions obtained were then treated as follow: saturation with Mg and K, solvation with glycerol of the Mg-saturated specimens and heating at 105 °C, 330 °C, 380 °C, and 550 °C of the K-saturated specimens. Oriented samples of the untreated and treated clay separates were analyzed by X-ray diffraction using a Philips PW 1830 diffractometer, using a Fe-filtered Co-Kα1 radiation and operating at 35 kV and 25 mA; the step size was 0.02° 2θ, and the scanning speed was 1 s per step.

1. Agnelli AE, et al. (2007) Features of some paleosols on the flanks of Etna volcano (Italy) and their origin. *Geoderma* 142:112–126.
2. Holliday VT (1989) The Blackwater Draw Formation (Quaternary): A 1.4 m.y. record of eolian sedimentation and soil formation on the Southern High Plains. *Geol Soc Am Bull* 101:1598–1607.
3. Lordkipanidze DL, et al. (2007) Postcranial evidence from early *Homo* from Dmanisi, Georgia. *Nature* 449:305–310.

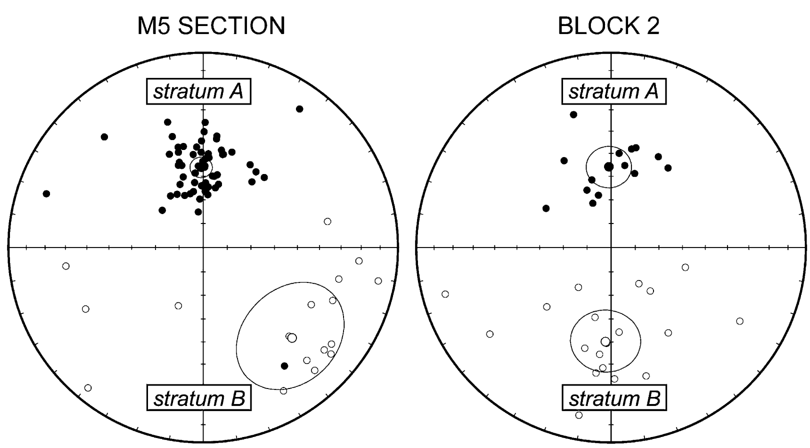

	N	dec	inc	K	a95
Reverse	17	135.4	-35.2	3.6	22.2
Normal	63	358.5	56.1	17.1	4.5

	N	dec	inc	K	a95
Reverse	19	183.4	-50.0	6.9	13.8
Normal	14	358.4	55.9	20.4	9.0

Fig. S1. Stereographic plots for the individual characteristic remnant magnetization values for M5 and block 2 sections (1). Empty and filled circles belong to the Southern and Northern hemispheres, respectively. Samples from stratum A display northern declinations and positive inclinations. Conversely, stratum B samples are southward-directed and show negative inclinations. Thus, the M5 section confirms the normal and reverse polarities observed in strata A and B, respectively. *n*, number of samples; decl., declination; incl., inclination; K and a95, Fisher statistic values.

1. Lordkipanidze DL, et al. (2007) Postcranial evidence from early *Homo* from Dmanisi, Georgia. *Nature* 449:305–310.

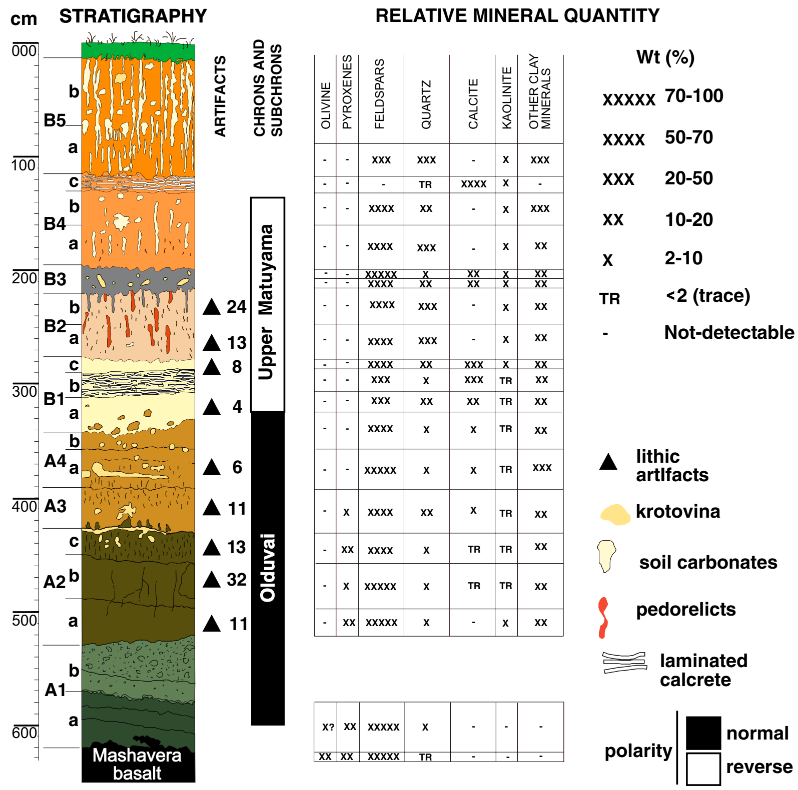

Fig. S2. Estimated relative abundance of crystalline mineral phases in the M5 deposits. The presence of olivine is evidence for minimal weathering of the Masavera Basalt and its rapid burial by A1a ashes. The upward declines in olivine and pyroxenes through stratum A suggest slower deposition and weak soil formation, although potential changes in sources of eolian sediment (volcanic and nonvolcanic) may be a factor as well. Overall, the mineralogy and morphology of the stratum A sediments and soils indicate cycles of episodic deposition interrupted by variable yet overall brief periods of surface stability and weathering. This pattern created an excellent site formation setting for the accumulation of the stratified assemblages recovered in M5.

Table S1. M5 profile description

Stratum	Depth below surface, cm	Description
B5	0–115	Brown (7.5YR4/4m) to yellowish brown (10YR5/6) silt loam; moderate medium prismatic structure, breaking to strong medium subangular blocky structure; common fine pores; many thick argillans (clay films); common fine mangans (MnO coatings) over argillans; many carbonate filaments and rare fine concretions; many coarse vertical masses of very pale brown (10YR7/4) pedogenic carbonate; many thick carbonate coats over argillans and mangans; diffuse, smooth boundary
B4	115–195	Dark yellowish brown (10YR3/4m) to brown (7.5YR4/4) silt loam; moderate fine subangular blocky structure; rare fine ferro-manganese stains; common vertical masses of pedogenic carbonate; upper 15-cm nodular and laminated petrocalcic horizon; abundant carbonate filaments and coats; common fine carbonate rhizoliths (root casts); abundant fine pores with clay and carbonate linings; many obsidian sand grains and rare granules; rare granule-sized rip-ups of A3 sediment in basal part; clear smooth boundary
B3	195–220	Grayish brown (10YR5/2m); medium and fine silt ash; massive; 50% black/50% clear obsidian; violent reaction to dilute HCl; many fine to medium pores with rare carbonate linings; many 2- to 2.5-cm krotovina (micromammal burrows), with soft, pale calcareous fills and hard carbonate linings; narrow tongues into subjacent B2 deposits; abrupt irregular boundary
B2b	220–245	Brown (7.5YR4/4m) silt loam; moderate medium subangular blocky structure; many medium argillans; few ferro-manganese stains; common fine pores; no reaction to HCl; abundant obsidian sand and rare granules; rare medium and fine sand grains of tuff and basalt; few krotovina with B3 fill; gradual smooth boundary
B2a	245–275	Strong brown (7.5YR4/6m) matrix-supported gravelly loamy sand to silt loam; vertical “pedorelicts” (in situ remnants of an argillic horizon, isolated by bioturbation) with strong fine subangular blocky structure; many fine to medium argillans; many ferromanganese stains; abundant fine pores with clay and carbonate linings; many carbonate filaments; common coarse sand to granule, black and clear obsidian grains; common well rounded, poorly sorted pebbles and cobbles of diverse lithology; clear smooth boundary
B1c	275–290	Brown (7.5YR5/4m) silt loam; massive; abundant fine pores, many with carbonate linings; violent reaction to HCl; abrupt smooth boundary
B1b	290–310	Pale brown (10YR6/3m); massive with secondary subhorizontal to anastomosing, indurated calcareous laminae; envelops darker sediment in small patches; many black coarse silt and fine sand obsidian clasts; many fine pores with carbonate linings; common carbonate filaments overprinting calcareous laminations; abrupt smooth boundary
B1a	310–340	Pale brown (10YR6/3m); massive calcareous silt ash; many coarse silt and fine sand glass shards, and few granules of obsidian, mainly black; few medium pores with carbonate linings; few to common fine (3- to 4-mm) subangular rip-ups of A4 sediment; few bioturbated coarse remnants of A4; common krotovina with soft calcareous fill and hard carbonate linings
A4b	340–355	Dark yellowish brown (10YR3/4m); massive silt; black, light tan, and clear obsidian clasts in sand-coarse silt fraction; few to rare fine pores with carbonate linings; few glass shards; few carbonate filaments; common krotovina with gray calcareous fill; abrupt wavy boundary
A4a	355–390	Very dark grayish brown (10YR3/2m) massive, friable coarse and medium silt; well rounded black, tan, and few reddish clasts, mainly obsidian; common fine pores with carbonate linings; many carbonate filaments; few medium rhizoliths; common krotovina with gray calcareous fill; abrupt wavy boundary
A3	390–430	Dark brown (7.5YR3/2.5m); massive fine silt; many carbonate filaments and coarse and medium pores with carbonate linings; tan and minor black clasts, mainly obsidian; few krotovina with soft, grayish brown calcareous fill; abrupt bioturbated boundary
A2c	430–455	Dark brown (7.5YR3/2m) coarse silt and fine sand ash; fine and medium subangular blocky structure; hard when dry; abundant coarse pores with carbonate linings, and many fine pores with and without linings; black glass shards predominate, with subordinate tan and clear obsidian; thick carbonate rinds on some ped surfaces; abrupt to clear wavy boundary
A2b	455–490	Dark reddish brown (8.75YR3/3m) in upper part and dark brown (7.5YR3/2) in lower part; very fine, fresh silt ash; moderate medium subangular blocky structure; very hard when dry; fresh black and subordinate clear obsidian in upper part, with many shards and tears in lower part; many fine and medium pores, rarely with pendant sparry calcite; few clay linings of larger pores in upper part, common in lower part; clay linings overlain by carbonate; few larger pores (2–5 mm), which frequently show bifurcations; rare krotovina with soft fill; abrupt wavy boundary
A2a	490–530	Very dark brown (10YR2.5/2m); very compact fine and medium silt ash; very hard when dry; fresh black, tan, and subordinate clear glass shards; moderate medium subangular blocky structure; many fine and few coarse pores with many thin to medium clay linings of fine pores only; no reaction to HCl in upper part, common carbonate filaments on ped surfaces and many medium calcareous rhizoliths and concretions in lower part; abrupt wavy boundary
A1b	530–570	Black (10YR2/1) to very dark brown (10YR2/2m) coarse sand and granules (~5%) in silt matrix; granules are well rounded clear and black obsidian, and rounded pumice clasts with frosted surfaces; common coarse pores with carbonate linings; abrupt wavy to irregular boundary

Table S1. Cont.

Stratum	Depth below surface, cm	Description
A1a2	570–590	Black (10YR2/1m); massive, friable moderately sorted fine sand and coarse silt ash with a few thin beds with fine laminations; black and clear obsidian shards and tears predominate, with many clear, rounded, unfrosted obsidian sand clasts; very rare granules of clear pumice with frosted surfaces; common fine, unlined pores, and few medium to large pores with carbonate linings
A1a1	590–620	Black (7.5YR2.5/1m); massive coarse silt and fine sand ash; subequal black and clear shards, with rare red obsidian and rare coarse sand to fine granule pumice with frosted surfaces; abundant fine unlined pores, and few medium to large pores with carbonate linings
Masavera Basalt	620	Black, fine-grained massive to vesicular basalt with sharp, fresh edges on blocky surface

Table S2. Soil morphologic features of M5 deposits

Stratum	Depth, cm	Munsell hue*	Color value/ chroma*	Texture[†]	Structure, G SC T[‡]	Illuvial clay, A L[§]	Soil carbonates, A T[¶]
B5	0–115	7.5YR	4/4	SiL-SiCL	3 m sab	3 pf	3 k, f, cc
B4	115–195	10YR	3/4	SiL-SiCL	2 f sab	3 po	3 k, f, r; K
B3	195–220	10YR	5/2	fSi ash	M		3 p
B2b	220–245	7.5YR	4/4	SiL	2 m sab	2 pf	N rctn
B2a	245–275	7.5YR	4/6	gr LS-SiL	3 f sab	2 pf	3 f, p
B1c	275–290	7.5YR	5/4	SiL	M		3 p
B1b	290–310	10YR	6/3	SiL	M		3 f, p; K-lam
B1a	310–340	10YR	6/3	cSi ash	M		1 p
A4b	340–355	10YR	3/4	cSi	M		1 f p
A4a	355–390	10YR	3/2	c, mSi	M		3 f, p, r
A3	390–430	7.5YR	3/2.5	fSi	M		3 f, p
A2c	430–455	7.5YR	3/2	cSi, fS ash	2 f sab		3 p, k
A2b	455–490	8.75YR	3/3	fSi ash	2 m sab	1 po	1 p, f
A2a	490–530	10YR	2.5/2	f, mSi ash	2 m sab	3 po	2 f, p; 3 r, cc
A1b	530–570	10YR	2/1	c LS	M		2 p
A1a2	570–590	10YR	2/1	fS, cSi ash	M		1 p
A1a1	590–620	7.5YR	2.5/1	cS, fS ash	M		1 p

*Munsell values in moist soil.
[†]SiL, silt loam; SiCL, silty clay loam; Si, silt; S, sand; gr, gravelly; c, coarse; f, fine.
[‡]G, grade: m, massive; 2, moderate; 3, strong. SC, size class: f, fine; m, medium. T, type: sab, subangular blocky.
[§]A, amount: 1, few; 2, common; 3, many. L, location: po, pore linings; pf, ped faces.
[¶]A, amount: 1, few; 2, common; 3, many. T, type: f, filaments; po, pore linings; k, coats; cc, concretions; r, rhizoliths.

Table S3. Cortex and dorsal scar patterns of flakes from M5, stratum B

Dorsal scar pattern	Platform only	Dorsal cortex, %				Sum
		None	1–50	50–99	100	
Cortex only					9	**9**
Unidirectional		9	9	5		**23**
Bidirectional			2			**2**
Opposed		1				**1**
Sum	**0**	**10**	**11**	**5**	**9**	**36**

Table S4. Cortex and dorsal scar patterns of flakes from M5, stratum A

Dorsal scar pattern	Platform only	Dorsal cortex, %				Sum
		None	1–50	50–99	100	
Cortex only					6	**6**
Unidirectional	3	34	2	7		**46**
Bidirectional		5	1			**6**
Opposed		1			1	
Platform removal	2	1			3	
Sum	**3**	**41**	**5**	**7**	**6**	**62**